Nanotechnology Perceptions
ISSN 1660-6795
www.nano-*ntp.com*

Tracking Fluid-Fluid Interface in Microchannels Using the Volume of Fluid Method

Sham Bansal[1], Ishu Goyal[2,*]

[1]*Department of Mathematics, Mata Gujri College, Fatehgarh Sahib, Punjab, India*
E-mail: shambansal2010@gmail.com
[2,*] *Department of Physics, Govt. Mohindra College, Patiala, Punjab, India.*
[*]*Corresponding Author E-mail: igoyal1986@gmail.com*

The current research investigates the two-phase flow of immiscible fluids passing a cylindrical obstruction. Numerical simulations were conducted using Ansys Fluent 17.0 to characterize the resulting flow patterns. The liquid-liquid interface was tracked using the Volume of Fluid (VOF) technique. The VOF multiphase flow model is effective in predicting the global behavior of liquid-liquid two-phase flows. In this work, two immiscible liquids with varying viscosities were made to flow adjacently in separate phases. The observed flow patterns were correlated with the Capillary and Reynolds numbers. The relatively low values of these parameters indicate a laminar flow regime where viscous forces and interfacial tension dictate the interface morphology. As a result, gravitational effects were deemed insignificant in this study, as the dominant forces within the model are viscous and surface tension forces. The results indicate a tendency for the more viscous fluid to move towards the less viscous fluid under the influence of viscous pressure, especially in the vicinity of the interface and on the surface of micro-particles, which are invariably surrounded by the liquid with higher viscosity.

Keywords: Two-phase, Liquid-liquid flow, Volume of fluid model, Interface.

1. Introduction

Two-phase flow, in the context of fluid mechanics, refers to the simultaneous flow of two distinct phases of matter. The occurrence of two-phase flow is widespread across numerous natural and engineered systems. For instance, in large-scale power generation, the heat transfer processes in boilers and nuclear reactors rely heavily on the behavior of two-phase mixtures of water and steam. The oil and gas industry routinely deals with the simultaneous flow of liquid hydrocarbons and natural gas in pipelines and processing equipment. In chemical engineering, many unit operations, such as distillation, absorption, evaporation, and condensation, involve multiphase flow phenomena. Environmental applications also frequently encounter two-phase flows, such as in the dispersion of pollutants in water or air and the aeration of rivers and oceans. The field of aerospace engineering utilizes the principles of two-phase flow in the design of rocket engines and for thermal management systems in spacecraft. Furthermore, emerging areas like biomedical engineering and microfluidics are increasingly relying on the understanding and manipulation of multiphase flows for applications ranging from targeted drug delivery to lab-on-a-chip devices. The two immiscible

liquids involved typically exhibit different thermophysical properties, such as density and viscosity, which directly influence their flow behavior. Surface tension, acting at the interface between the liquids, plays a crucial role in interfacial phenomena, affecting the shape and stability of the interface and leading to capillary effects.

Computational Fluid Dynamics (CFD) is a powerful numerical tool used to simulate fluid flow problems by discretizing the governing equations of fluid motion over a computational domain and solving them using numerical algorithms. One of the most common discretization techniques employed in CFD, including in software packages like Ansys Fluent, is the finite volume method (FVM). The FVM involves dividing the computational domain into a finite number of control volumes and then integrating the governing equations over each volume to obtain a system of algebraic equations that can be solved numerically. [1] developed a combined VOF and two-fluid method for simulating multiphase flows at multiple scales. This approach integrates algebraic VOF, interfacial force models, and a level-set technique to precisely track the movement of both large and small interfaces within multiphase systems. The simplified volume-of-fluid technique was implemented by [2] for tracking interfaces on adaptive Cartesian meshes. This approach is designed to precisely compute fluxes between computational cells with varying levels of refinement, ensuring stable, conservative, and accurate tracking of the interface. [3] explored a two-phase flow within a microchannel. The experimental setup involved deionized water and sunflower oil as the two liquid phases within a Y-shaped microchannel. [4] explored a geometric VOF approach to track the boundaries between different fluids. This method incorporated a novel interpolation algorithm designed for overset grids, enabling effective interface reconstruction within fringe cells and improving precision in scenarios involving intricate shapes and significant air-water interaction. [5] explored a computational approach for simulating two-phase flow. This approach integrated the incompressible smoothed particle hydrodynamics (ISPH) technique with the finite volume method. [6] investigated the diffusion of a submarine oil spill using a two-phase flow model. This model incorporated the VOF technique to track the oil-water interface. [7] utilized the VOF model to monitor the fluid-fluid interface in a microchannel reactor. This enabled the prediction of microdroplet sizes and advanced the understanding of multiphase flow patterns, critical for enhancing chemical reaction efficiency. A mathematical model, developed by [8], was used to forecast the angle of protrusion at a defined distance from the microchannel's entry point. This model was then integrated into CFD simulations to establish the fixed shape of the interface, a shape that changes as one moves along the channel's length.

The problem of fluid flow past a cylindrical object is a fundamental benchmark in fluid dynamics, extensively studied due to its relatively simple geometry yet its ability to exhibit a wide range of flow phenomena depending on the Reynolds number. A key phenomenon observed in flow past a cylinder is the development of the Karman vortex street at certain Reynolds numbers, which is a pattern of alternating vortices shed from the cylinder, indicating unsteady flow in the wake region. [9] conducted a numerical comparison of two-phase flow around a solitary cylinder across a range of Reynolds numbers. Their investigation explored the development of the vortex field and detailed the characteristics of the flow field, the pattern of vortex shedding, and the resulting drag and lift forces on the cylinder. [10] examined the influence of introducing dust particles into a compressible gas flow. The research indicated that this particle seeding generates disturbances within the flow and results in higher skin friction and drag coefficients. Furthermore, the study found that larger particles contribute to

greater flow instability, while smaller particles increase drag through collisional effects. [11] detailed an investigation into the dynamics of multiphase flow around a two-dimensional cylinder, employing a GPU-accelerated Lattice Boltzmann Method. The study further explored the connection between the extreme values of various vortex identification parameters and the process by which droplets change shape. [12] utilized simulations of two-phase flow to study scour around cylinders positioned both horizontally and vertically. Their research specifically examined how vortices affected the transport of sediment, and the results indicated that the model employed was effective in numerically reproducing the dynamics of scour.

The flow pattern around a cylinder is strongly dependent on the Reynolds number, which represents the ratio of inertial forces to viscous forces in the fluid. At very low Reynolds numbers (Re << 1), the flow is dominated by viscous forces, resulting in a steady, symmetrical flow where the fluid streamlines closely follow the shape of the cylinder. Viscous forces and interfacial tension are two fundamental physical phenomena that play a critical role in determining the behavior of immiscible liquids. [13] offered a comprehensive analysis of interfacial momentum transfer models, emphasizing their importance because computational fluid dynamics in most two-phase flow systems is primarily governed by interfacial structures and the transfer of momentum across these interfaces. [14] examined how capillary and viscous forces affect the movement of two immiscible fluids within microfluidic devices. Their findings illustrated that the patterns and effectiveness of this displacement process varied based on the viscosity ratio between the fluids and the capillary number. Furthermore, the researchers introduced a theoretical framework to describe different modes of fluid invasion. [15] pointed out the substantial impact of interfacial tension on the dimensions of droplets and the patterns of flow observed in viscous multiphase systems. Their findings indicate that a decrease in interfacial tension results in the formation of smaller droplets, underscoring the vital part played by these effects in the behavior of two-phase flows. In two-phase flow involving immiscible liquids, viscous forces and interfacial tension are key factors shaping phenomena like wetting, droplet formation, and stability. These aspects are essential for applications in emulsion technology and fluid dynamics, as documented in [16]. [17] detailed the interplay between viscous and interfacial tension forces, highlighting how co-moving and average seepage velocities influence fluid behavior as pressure gradients and saturation levels change.

1.1 Governing Equations

In the present work, the equations used are the Incompressible Navier-Stokes Equations which
In the present work, the equations used are the Incompressible Navier-Stokes Equations which comprise of the continuity equation and momentum equation. The equation of continuity is a statement of mass conservation. Its general form is

$$\frac{\partial \rho}{\partial t} + \nabla . \left(\rho \vec{v} \right) = 0 \tag{1}$$

Where ρ is density and $\vec{v}$ is velocity vector. Under the assumption of incompressibility, the density of a fluid is constant and it follows that the continuity equation (1) will simplify to:

$$\nabla . \vec{v} = 0 \tag{2}$$

A single momentum equation has been solved throughout the domain using volume of fluid model, and the resulting velocity field is shared among the phases. Because the fluids do not mix, each computational cell is filled with purely one fluid and purely another fluid or the

interface between two (or more) fluids. Because of this unique set of conditions, only a single set of Navier-Stokes equations is required. The momentum equation shown below, is dependent on the volume fractions of all phases through the properties μ and ρ.

$$\rho\left[\frac{\partial v}{\partial t}+\vec{v}\nabla.\vec{v}\right]=-\nabla p+\mu\nabla^2\vec{v}+\rho g+\vec{F} \tag{3}$$

Where p is the pressure, μ is the viscosity, g is the gravitational force and F an additional body force.

In the present work, effect of gravity force has been neglected because it has very less effect compared to viscous and surface tension forces and Continuity and Momentum equations have been reduced to dimensionless form. New dimensionless variables have been defined:

$$\tilde{v}=\frac{v}{V},\quad \tilde{t}=\frac{\mu}{\rho L^2}t,\quad \tilde{p}=\frac{L}{\mu V}p,\ \tilde{x}=\frac{x}{L},\quad \tilde{y}=\frac{y}{L},\quad \tilde{F}=\frac{L^2}{\mu V}F \tag{4}$$

Therefore, Continuity and Momentum equations in dimensionless form, become

$$\tilde{\nabla}.\tilde{v}=0\quad\text{and}\quad\frac{\partial\tilde{v}}{\partial\tilde{t}}=-\tilde{\nabla}\tilde{p}+\tilde{\nabla}^2\tilde{v}+\tilde{F} \tag{5}$$

It is known as instationary stokes equation.

2. NUMERICAL METHODOLOGY

Numerical methodology in Fluent to solve the problem is quite good. It follows some algorithms to solve the problem.

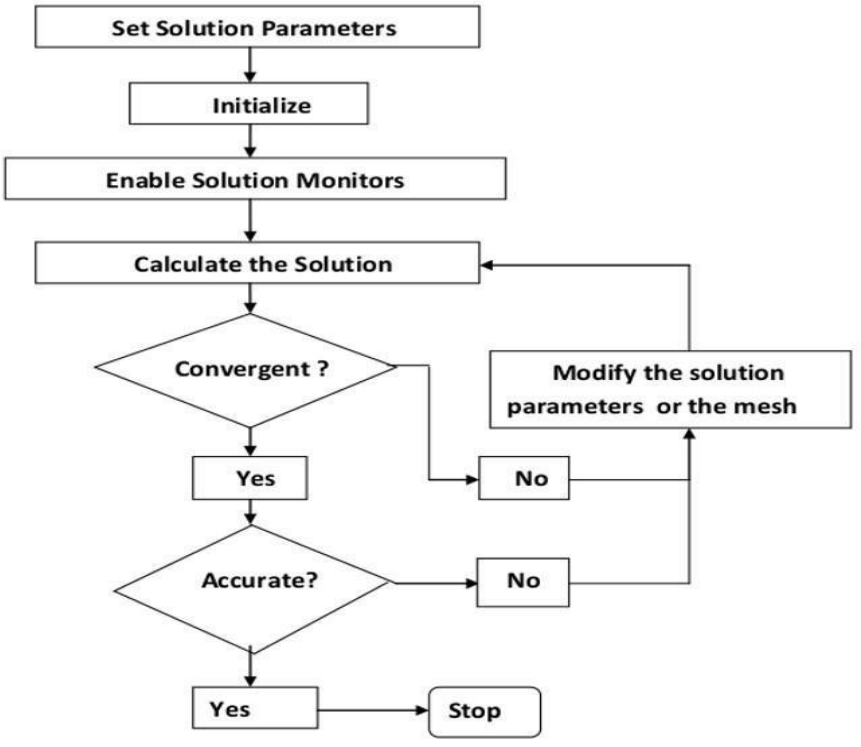

Figure 1: Flowchart showing the general procedure for the simulation using Fluent

There are number of options of different methods that can be selected according to our model. Our problem is based on two phases. These two phases are called Primary and Secondary phases. Volume of fluid model uses the single set of momentum equations to solve the problem. The solution convergence depends upon the parameters and meshing. If either of parameters or meshing is not correct then solution may diverge or may give a poor convergence. The model equations have been solved using the commercial CFD software package Ansys Fluent 17.0. Figure 1 shows the general procedure for the simulation using Ansys Fluent software.

2.1 Geometry and Mesh

The first step is to create the geometry, which has been done by DM (Design Modular) tools in Ansys, to design the problem in geometrical configuration and mesh the geometry. Before using Fluent, one has to solve the fluid flow problems, it needs the domain in which the flow takes place to evaluate the solution. The flow domains as well as the grid generation into the specific domain have been created in Design Modular. Two-dimensional geometry has been created and meshed to form the grid. In order to create the desired geometry, firstly the surface body for the cylinder particle has been created, and then the surface body for the outer boundary was built. In two-dimensional geometry triangular and quadrilateral meshing techniques have been used to mesh the geometry. The boundary conditions such as velocity-inlet, pressure outlet, symmetry and default interior have been set. Then the grid has been exported as a mesh file from DM to be used in Ansys Fluent 17.0 for solution. Next, after meshing the geometry, mesh size is defined as: 11,826 elements, 18,442 faces and 12,504 nodes (See Figure 2).

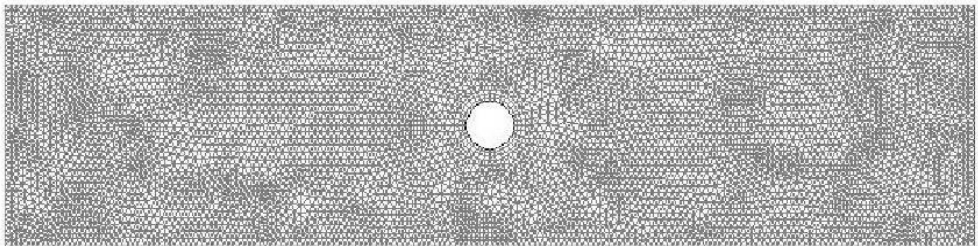

Figure 2: Mesh size: 11,826 elements, 18,442 faces and 12,504 nodes

2.2 Boundary and initial conditions

In present work, we have implemented reasonable boundary conditions for the computational domain. The diameter of cylinder particle has been taken as $D = 200\mu m$. The length of calculation domain is taken to be 20 times of the diameter, i.e. $L = 4000\mu m$ and the height is considered as 5 times of the diameter, i.e. $H = 1000\mu m$. Inlet-velocity boundary condition for both the liquids is $u_x = 0{:}\ 001(m/s)$ and $u_y = 0(m/s)$. Outlet boundary condition is pressure-outlet boundary condition, which has been set as 0 Pascal (Pa). Wall boundary condition is no-slip boundary condition, which has already defined. Boundary conditions are shown in Figure 3

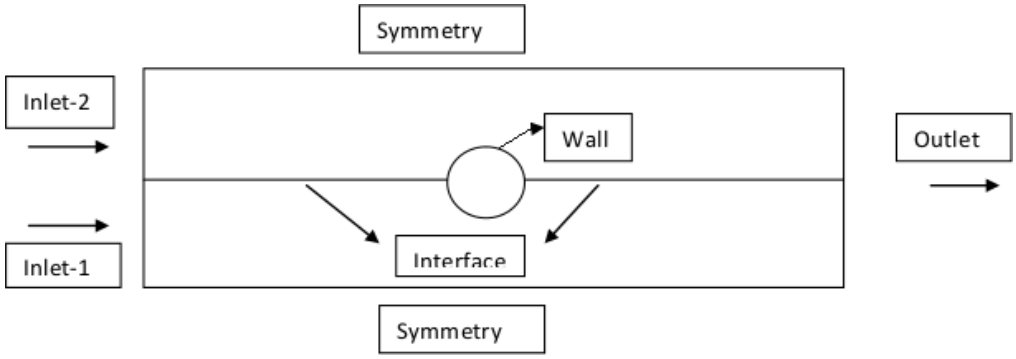

Figure 3: Calculation domain with boundary conditions

2.3 Solution Techniques

In Fluent, solver has been set as segregated which solves the equations individually. First order implicit condition and node based gradient option has been taken. The discretization scheme for momentum has been taken as second order upwind and the discretization scheme for volume fraction geometric reconstruction has been taken. The solution procedure involves the following steps:

- Generation of suitable grid system.
- Conversion of governing equation into algebraic equations.
- Selection of discretization schemes.
- Formulation of the discretized equation at every grid location.
- Formulation of pressure equation.
- Development of a suitable iteration scheme for obtaining a final solution.

3. Results and Discussion

In the present work, velocity $U = 0.001(m/s)$, diameter of cylinder particle $D = 0.0002m$ and the viscosities of liquid-1 and liquid-2 have been taken in the range $0.001(kg/ms)\ to\ 0.0024(kg/ms)$. The densities of liquid-1 and liquid-2 have been taken in the range $780(kg/m^3)\ to\ 998.2(kg/m^3)$.

For this particular model, the dimensionless numbers are:

$$Re << 1,\quad Ca << 1 \quad \text{and} \quad We << 1$$

Then inertial forces can be neglected, viscous forces play a dominant role and flow is laminar for such a Reynolds number. Surface tension forces also play important roles in the system as Ca and We are very low. Therefore, viscous forces and surface tension forces are the main

dominant forces in the present model. Therefore, gravity force can be neglected because it is very less effective as compared to viscous and surface tension forces. So, the gravity force in the present work has been neglected. The surface tension between two liquids has been taken as $\sigma = 0.001(N/m)$ and the contact angle, at which liquid-1 and liquid-2 interface meets the cylinder particle, has been taken as 90^0. Liquid-1 has been considered as water and liquid-2 can be any other liquid with different viscosity. In the present study, the ratio of viscosities of two liquids have been considered, which is defined as $\beta = \mu_2 / \mu_1$ where μ_1 and μ_2 are viscosities of liquid-1 and liquid-2 respectively. Then three cases are possible.

$$\mathbf{1}.\ \beta = 1 \qquad \mathbf{2}.\ \beta > 1 \qquad \mathbf{3}.\ \beta < 1$$

Case-I: When $\beta = 1$, all the parameters of both the liquids are same in this case. Liquid-1 is considered as water and therefore: $\rho_1 = \rho_2 = 998.2\ kg/m^3\ and\ \mu_1 = \mu_2 = 0.001 kg/ms$ Where ρ_1 and ρ_2 are densities of liquid-1 and liquid-2 respectively. After running some time steps with time step size $0.0005\ (s)$, it has been observed that there is no change in the shape of interface and fluid is moving smoothly over the cylinder particle as in single- phase problem. So when there is no change in flow then the calculation has been stopped after 2,000 time steps with time step size $0.0005\ (s)$. See Fig.4, there is no change in the shape of interface.

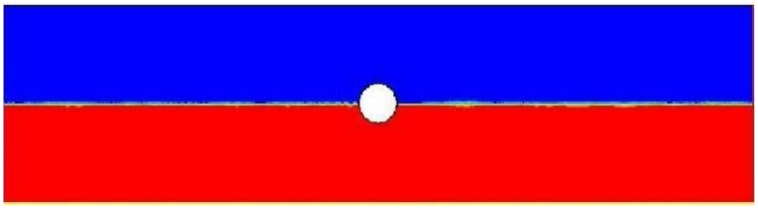

Figure 4: Contour volume fraction of liquid-1, after 2,000 time steps with step size 0.0005(s)

Case-II: When $\beta > 1$, for liquid-2, the viscosity has been taken as $\mu_2 = 0.0024\ (kg/ms)$. Therefore:

$$\rho_1 = 998.2(kg/m^3),\ \mu_1 = 0.001(kg/ms),$$
$$\rho_2 = 998.2(kg/m^3),\ \mu_2 = 0.0024(kg/ms)$$

In this case, after some iteration it has been observed that interface started moving towards liquid-1 because of the high viscous pressure of liquid-2 at the wall of cylinder particle near interface in the presence of interfacial force. Therefore, interface started moving towards liquid-1. Viscous pressure difference of two liquids and capillary pressure are:

$$\Delta P_v = \frac{\mu_2 U_2}{R} - \frac{\mu_1 U_1}{R} \qquad and \qquad \Delta P_c = \frac{\sigma}{R} \tag{6}$$

Where U_1 and U_2 are velocities of liquid-1 and liquid-2 respectively and R is radius of cylinder particle. Here, velocity of both liquids is same and $\mu_2 > \mu_1$. It implies there is some positive viscous pressure on the wall of cylinder near the interface and hence it started moving towards liquid-1, which is less viscous. Then the interface detaches from the cylinder particle (See Figures 5, 6, 7 and 8)

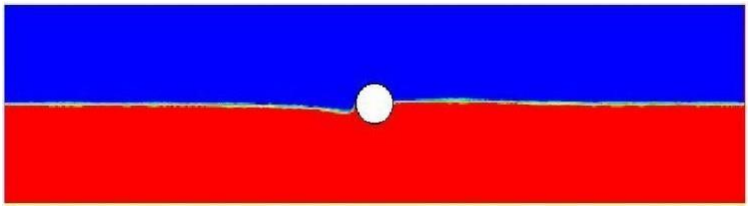

Figure 5: Contour volume fraction of liquid-1, after 5,00 time steps with step size 0.0005(s)

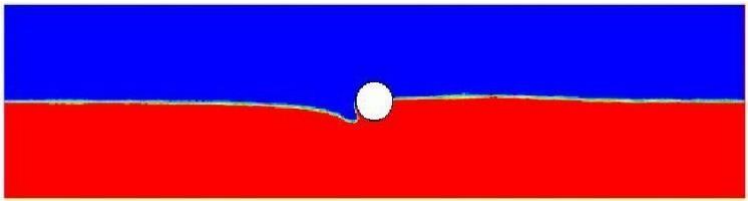

Figure 6: Contour volume fraction of liquid-1, after 1,000 time steps with step size 0.0005(s)

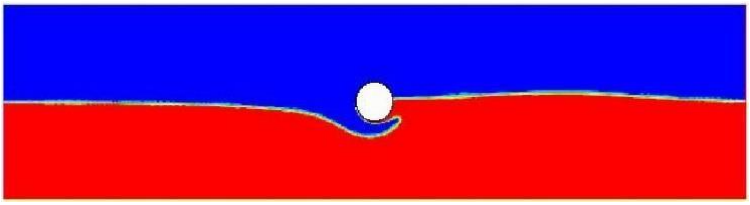

Figure 7: Contour volume fraction of liquid-1, after 2,000 time steps with step size 0.0005(s)

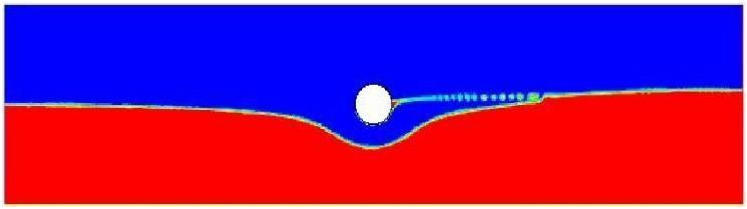

Figure 8: Contour volume fraction of liquid-1, after 5,000 time steps with step size 0.0005(s)

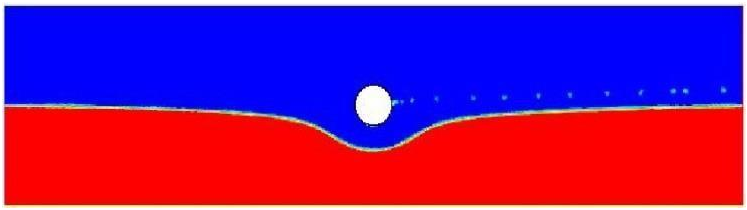

Figure 9: Contour volume fraction of liquid-1, after 10,000 time steps with step size 0.0005(s)

After running the $10{,}000$ time steps with time step size $0.0005s$, it has been observed that there is no more change in flow and in the shape of interface. It indicates that flow has come to quasi steady state. (Figure 9)

Case-III: When $\beta < 1$, for liquid-1, the viscosity has been taken as $\mu_2 = 0.0024\ (kg/ms)$. Therefore:

$$\rho_1 = 998.2(kg/m^3),\ \mu_1 = 0.0024(kg/ms),$$
$$\rho_2 = 998.2(kg/m^3),\ \mu_2 = 0.001(kg/ms)$$

After some iterations, it has been observed that interface started moving towards liquid-2 because of the high viscosity pressure of liquid-1 at the wall of cylinder particle near interface in the presence of interfacial force. It implies there is some negative viscous pressure on the wall of cylinder particle near the interface, so its direction is opposite now and hence it started moving towards liquid-2 and then the interface detaches from the cylinder particle. After running the $10{,}000$ time steps with time step size $0.0005s$, it has been observed that there is no more change in flow and interface. This implies that flow has come to quasi steady state. (See Figure 10)

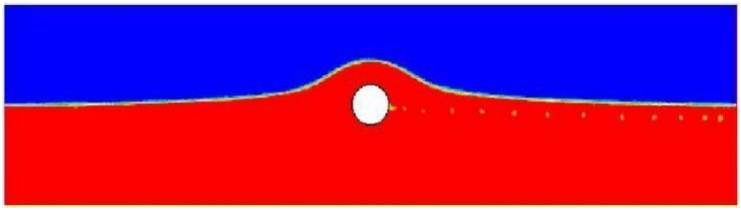

Figure 10: Contour volume fraction of liquid-1, after $10{,}000$ time steps with step size $0.0005(s)$

In another case, when densities of liquid-1 and liquid-2 are different and viscosities are same, then no effect of density has been observed and fluid flows smoothly over the cylinder particle as in single-phase problem.

Now, if $\beta > 1$ as mentioned in the Case-II, has been further investigated. Here, viscosity of one liquid has been fixed and the viscosity of other liquid has varied. Liquid-1 has been taken as water and liquid-2 can be any other liquid with different viscosity. Now consider: In this case, after some iterations, it has been observed that there is small viscous pressure of liquid-2 on the wall of cylinder near interface in the presence of interfacial force and interface started moving towards liquid-1. In this case viscous pressure difference is very low. Therefore, the interface covered the less space in phase-2. See Figure 11

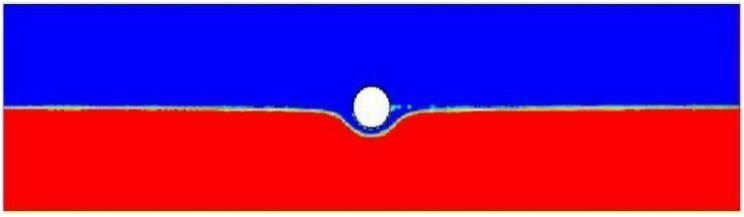

Figure 11: Contour of volume fraction for liquid-1, after $10{,}000$ time steps with step size $0.0005(s)$, when $\mu_1 = 0.001\ (kg/ms)$ and $\mu_2 = 0.0011\ (kg/ms)$.

Now, the viscosity of liquid-2 has been changed to $\mu_2 = 0.0015\ (kg/ms)$. This time, it has been observed that there is little more viscous pressure of liquid-2 as compared to the case when $\mu_2 = 0.0011\ (kg/ms)$. It is because the viscous pressure is increasing, which creates more pressure on the cylinder wall near the interphase. Now liquid-2 covered little more space in phase-1. See Figure 12

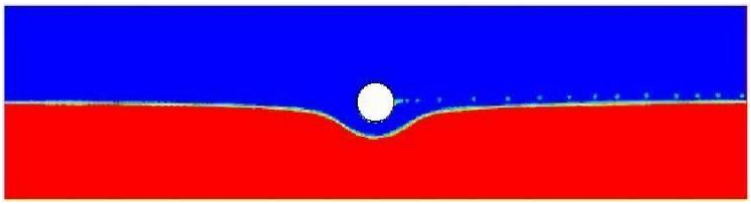

Figure 12: Contour of volume fraction for liquid-1, after $10{,}000$ time steps with step size $0.0005(s)$, when $\mu_1 = 0.001\ (kg/ms)$ and $\mu_2 = 0.0015\ (kg/ms)$.

Hence, it is concluded that when the viscosity of liquid-2 has been increased then viscous pressure has increased on the wall of cylinder particle near the interface and liquid-2 covered more space in phase-1.

Table 1 Variation of length of δ with respect to increase in difference of liquid's viscosities and increment in length of δ per unit radius length of cylinder particle.

μ_1	μ_2	$\beta = \mu_2 / \mu_1$	δ	δ / R
0.001	0.001	1	0	0
0.001	0.0011	1.1	$3.35e^{-5}$	0.335
0.001	0.0012	1.2	$4.65e^{-5}$	0.465
0.001	0.0013	1.3	$5.75e^{-5}$	0.575
0.001	0.0014	1.4	$6.65e^{-5}$	0.665
0.001	0.0015	1.5	$7.40e^{-5}$	0.740
0.001	0.0016	1.6	$8.10e^{-5}$	0.810
0.001	0.0017	1.7	$8.75e^{-5}$	0.875
0.001	0.0018	1.8	$9.40e^{-5}$	0.940
0.001	0.0019	1.9	$1.00e^{-4}$	1
0.001	0.0020	2.0	$1.055e^{-4}$	1.055
0.001	0.0021	2.1	$1.105e^{-4}$	1.105

0.001	0.0022	2.2	$1.150e^{-4}$	1.150
0.001	0.0023	2.3	$1.195e^{-4}$	1.195
0.001	0.0024	2.4	$1.235e^{-4}$	1.235
0.001	0.0024	2.5	$1.265e^{-4}$	1.265
0.001	0.0026	2.6	$1.295e^{-4}$	1.295
0.001	0.0027	2.7	$1.325e^{-4}$	1.325

The length between interface and the wall of cylinder particle (from bottom) has been taken as δ and this δ increases by increasing the viscosity of liquid-2. On this basis a table has been constructed which represents the increment in δ with respect to viscosity. See Table1 which indicates that if viscosity difference is increasing then the increment length δ is also increasing, but the rate of increment of the length δ is decreasing. The increment in length δ per unit radius length of cylinder particle has been computed, which provides more clear view. The graph of $\beta = \mu_2/\mu_1$ and the increment length δ per unit radius length of the cylinder particle has been plotted in Figure 13

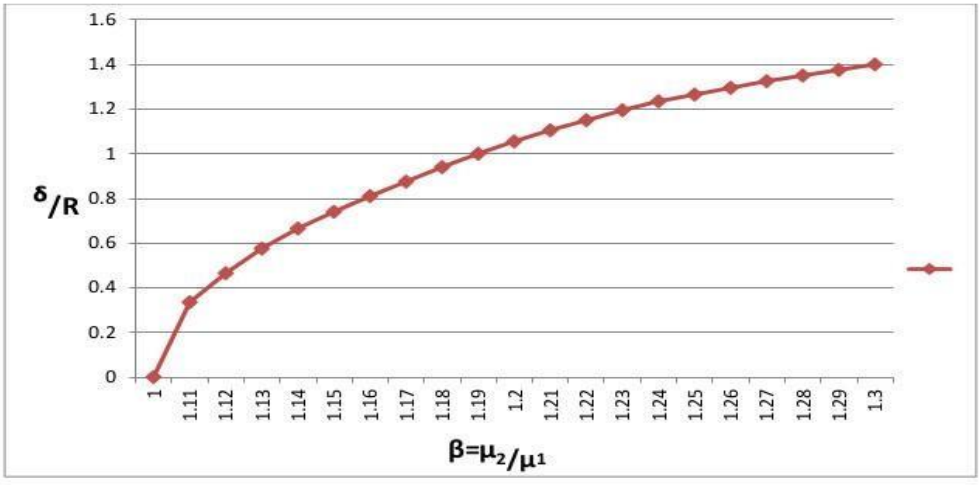

Figure 13: Graph of $\beta = \mu_2 / \mu_1$ and the increment length δ per unit radius length of the cylinder particle.

From Figure 13 it is clearer that the increment length per unit radius increases with increase in difference of the viscosities. But it has been also observed from the graph that initially there is more increment in the length δ per unit radius of particle and the rate of increment decreases with the length of δ per unit radius of the particle.

In the present work, it has also been observed that all the results are grid independent. Firstly, the geometry has been meshed with 11,826 elements, 18,442 faces and 12,504 nodes and then the model has been simulated using this grid size. Then the mesh has been refined with mesh

size 90,624 elements, 1,37,020 faces and 93,000 nodes. Then the model has been simulated again using this grid-size. It has been observed that results are same with sharper interface. Results are not affected by increasing the grid size. It implies that results are grid-independent. On the basis of these two different grid sizes, contour of volume fractions of each of the cases with $\mu_1 = 0.001(kg/ms)$, $\mu_2 = 0.002(kg/ms)$ and $\rho_1 = \rho_2 = 998.2(\ kg/m^3\ )$ is shown in Figures 14 and 15 respectively.

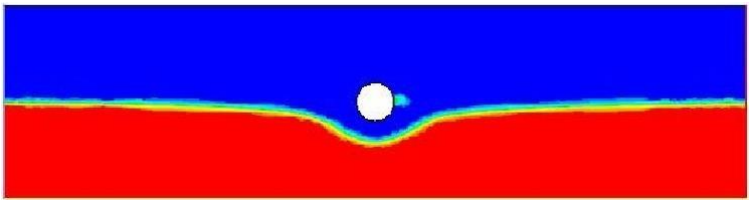

Figure 14: Contour of volume fraction for liquid-1 with mesh size 11,826 elements, 18,442 faces and 12,504 nodes, after running the 10,000 time steps with time step size $\mathbf{0.001}(\boldsymbol{s})$

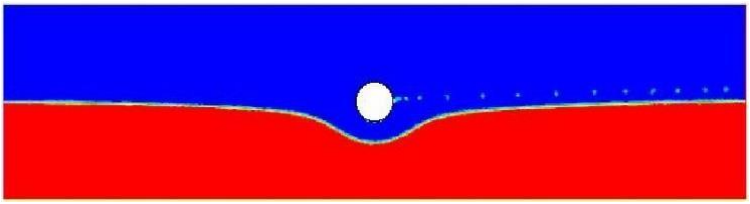

Figure 15: Contour of volume fraction for liquid-1 with mesh size 90,624 elements, 1,37,020 faces and 93,000 nodes, after running the 10,000 time steps with time step size $\mathbf{0.0005}(\boldsymbol{s})$

From figures, it can be observed that by increasing the number of elements interphase becomes sharper. But there is no difference in results, even the increment δ is same for all the three different grid sizes. Therefore, results are grid-independent.

4. Conclusion

In this work, a report on movement of micro-particles at fluid-fluid interface has been studied. Results have been obtained by using VOF method in Ansys fluent 17.0 software. Results have been discussed on basis of different fluid properties. The dimensionless numbers $Re,\ Ca,\ and\ We$ are very small compared to unity. Therefore, inertial forces can be neglected. Viscous forces and surface tension forces are the main dominant forces in the model. Obtained are the following conclusions:

1. Particle is always covered by high viscosity liquid. More viscous fluid moves towards the less viscous fluid in the presence of viscous pressure and on the wall of micro particle near the interface.
2. If the viscosities of both the fluids are equal and densities are different, then there is no change in shape of interface and fluid flows in the same pattern as in the single-phase flow.

3. If the fluids in two-phases have been interchanged, it has been found that the direction of interface also changes.
4. When difference of viscosities of two fluids is less, then the more viscous fluid covers the less space in the less viscous fluid phase.
5. If the difference of viscosities of the two fluids increased then the space covered by more viscous fluid in the less viscous fluid phase also increased.
6. The rate of increment in space, covered by the more viscous fluid in the less viscous fluid phase, decreased by increasing the difference in viscosities of two fluids.
7. Results are grid-independent, because after refining the mesh up to 90,624 elements, there is no change in the results.

The current research highlights potential uses in the realm of paints and surface treatments. Specifically, paints exhibiting a greater viscosity than water could be valuable for marine environments. This implies that the findings could be leveraged to coat ships, thereby offering protection against corrosion caused by seawater. The study's results indicate that the high- viscosity liquid consistently encapsulates the particle. Consequently, a paint with a higher viscosity than water is anticipated to create a barrier that prevents water from reacting with the surface.

Conflict of Interest: The authors declare no conflicts of interest.

Data Availability: Data will be made available on reasonable request.

REFERENCES

[1] Park, J., & Son, G. (2023). Multiscale Simulation of Multiphase Flow Using a Coupled VOF And 2-Fluid Method. Journal of Computational Fluids Engineering, 28(4), 92–97. https://doi.org/10.6112/kscfe.2023.28.4.092

[2] G. T. Suwito, J. Vorspohl and E. Juntasaro, "A Simplified Volume of Fluid Method for Interface Tracking on Adaptive Cartesian Grids," 2023 Research, Invention, and Innovation Congress: Innovative Electricals and Electronics (RI2C), Bangkok, Thailand, 2023, pp. 229-234, https://doi.org/10.1109/RI2C60382.2023.10356018.

[3] E. Chiriac, A. M. Bran, C. Voitincu and C. Balan, "Experimental Validation of VOF Method in Microchannel Flows," 2021 12th International Symposium on Advanced Topics in Electrical Engineering (ATEE), Bucharest, Romania, 2021, pp. 1-4, https://doi.org/10.1109/ATEE52255.2021.9425121.

[4] Wang, Z., & Stern, F. (2022). Volume-of-fluid based two-phase flow methods on structured multiblock and overset grids. International Journal for Numerical Methods in Fluids, 94(6), 557–582. https://doi.org/10.1002/fld.5066

[5] Xu, Y., Yang, G., & Hu, D. (2022). An ISPH-FVM coupling algorithm for interface tracking of two-phase fluid flows. International Journal for Numerical Methods in Fluids, 94(9), 1434–1464. https://doi.org/10.1002/fld.5094

[6] Liu, R., Ding, S., & Ju, G. (2022). Numerical Study of Leakage and Diffusion of Underwater Oil Spill by Using Volume-of-Fluid (VOF) Technique and Remediation Strategies for Clean-Up. Processes, 10(11), 2338. https://doi.org/10.3390/pr10112338

[7] Laziz, A. M., & Shaari, K. Z. K. (2020). Effect of Flow Regime on Total Interfacial Area of Two Immiscible Fluids in Microchannel Reactor Using VOF Model (pp. 585–597). Springer, Singapore. https://doi.org/10.1007/978-981-13-8297-0_61

[8] Qiu, J., Hudson, D. A., & Price, W. G. (2022). A Combined Volume of Fluid and Immersed Boundary Method for Modeling of Two-Phase Flows With High Density Ratio. Journal of Fluids Engineering-Transactions of The Asme, 144(3). https://doi.org/10.1115/1.4052242

[9] Chen, Z., Chen, P., Huang, X., Zhang, X., Gui, N., Yang, X., Tu, J., & Jiang, S. (2023). Numerical simulation and analysis of Two-Phase flow around cylinder using Pseudo-Potential model and Liutex method. Springer Proceedings in Physics, 288, 191–209. https://doi.org/10.1007/978-981-19-8955-1_13

[10] Wangikar, A. U., Bajpai, A., & Kumar, R. (2023). Supersonic dusty gas flow past a cylinder in Eulerian–Lagrangian framework. Physics of Fluids, 35(12). https://doi.org/10.1063/5.0174388

[11] Cheng, P., Gui, N., Yang, X., Tu, J., Jiang, S., & Jia, H. (2021). Liutex-Based Investigation of Vortex in Multiphase Flow Past 2-D Cylinder Using GPU-Accelerated LBM (pp. 123–137). Springer, Cham. https://doi.org/10.1007/978-3-030-70217-5_7

[12] Nagel, T., Chauchat, J., Bonamy, C., Mathieu, A., Liu, X., Cheng, Z., & Hsu, T.-J. (2018). Two-phase flow simulations of scour around vertical and horizontal cylinders. 1(36), 22. https://doi.org/10.9753/ICCE.V36.SEDIMENT.22

[13] Li, F., Kinoshita, H., Li, X., Oishi, M., Fujii, T., & Oshima, M. (2009). Creation of very-low-Reynolds-number chaotic fluid motions in microchannels using viscoelastic surfactant solution. Experimental Thermal and Fluid Science, 34(1), 20–27. https://doi.org/10.1016/j.expthermflusci.2009.08.007

[14] Chen, K., Liu, P., Wang, W., Chen, Y., & Bate, B. (2023). Effects of capillary and viscous forces on Two-Phase fluid displacement in the microfluidic model. Energy & Fuels, 37(22), 17263–17276. https://doi.org/10.1021/acs.energyfuels.3c03170

[15] Dinh, T., & Cubaud, T. (2021). Role of Interfacial Tension on Viscous Multiphase Flows in Coaxial Microfluidic Channels. Langmuir, 37(24), 7420–7429. https://doi.org/10.1021/ACS.LANGMUIR. 1C00782

[16] Honaker, L. W., Lagerwall, J. P. F., & Jampani, V. S. R. (2018). Microfluidic Tensiometry Technique for the Characterization of the Interfacial Tension between Immiscible Liquids. Langmuir, 34(7), 2403–2409. https://doi.org/10.1021/ACS.LANGMUIR.7B03494

[17] Roy, S. (2022). The Co-Moving Velocity in Immiscible Two-Phase Flow in Porous Media. Transport in Porous Media, 143(1), 69–102. https://doi.org/10.1007/s11242-022-01783-7